RSC Advances

PAPER

View Article Online
View Journal | View Issue

Open Access Article. Published on 11 September 2020. Downloaded on 12/4/2025 4:19:03 PM.
This article is licensed under a Creative Commons Attribution-NonCommercial 3.0 Unported Licence.

Check for updates

Cite this: *RSC Adv.*, 2020, **10**, 33675

Fabrication of microcapsule-type composites with the capability of underwater self-healing and damage visualization†

Hengyu Feng, Fei Yu, Yu Zhou, Ming Li,* Linghan Xiao* and Yuhui Ao

Inspired by biology, underwater self-healing polymer composites with damage-healing visible agents were successfully designed and prepared. The healing agents, same as epoxy resin matrices, were encapsulated and embedded into a matrix that contained fluorescent latent curing agents. The results of investigation on healing properties revealed that the fluorescent latent curing agents and the microcapsules in the matrix play two roles. First, the matrix could be self-healed *via* a crosslinking reaction between the amine group and epoxy resin, in which the amine group could be released from the fluorescent latent curing agents (FLCAs) after exposure to water. Second, the fluorescent dyes released under water could indicate the scratches and healing area visually. Embedding 15 mass% microcapsules and 6 mass% FLCAs in self-healing materials yielded a healing efficiency of 85.6% and the most efficient fluorescence detection. Self-healing materials can be repaired underwater and they show the location of damage, which is of great significance in applications such as water conservation engineering, environmental treatment engineering, ship engineering and ocean engineering.

Received 9th April 2020
Accepted 11th August 2020

DOI: 10.1039/d0ra03197f

rsc.li/rsc-advances

1 Introduction

The property of self-healing plays an important role in improving the safety of structures and extending their service life, especially in applications such as underground pipeline transportation and marine engineering.[1,2] Moreover, cracks tend to occur in dark environments and are difficult to view. Therefore, it is crucial to detect and repair any damage in advance to protect materials.[3–5] Inspired by the self-healing function of natural organisms, researchers have designed materials that can retain functionalities and restore their structure automatically after damage to improve the service and safety life of materials.[6,7] Thus, self-healing materials have attracted great attention and resulted in a certain degree of progress in the past decade.[8–10] Considering the long-term use of materials in high humidity environment or underwater is inevitable. Therefore, the stability of self-healing materials underwater has been recognized as necessary.[11–13]

Among external self-healing materials, microcapsule-embedded self-healing materials are much more popular for investigation due to their outstanding mechanical properties and simple operation.[14] White *et al.*[15] first applied microcapsule technology to material design and developed an intelligent self-healing material, which contained embedded encapsulated dicyclopentadiene (DCPD) and Grubbs catalyst in an epoxy resin matrix. In addition, fracture experiments yielded as much as 75% recovery in toughness. Since then, researchers have developed various microcapsule-type self-healing materials such as epoxy resin,[16] polydimethylsiloxane[17] glycidyl methacrylate[18,19] and tung oil.[20] Moreover, most self-healing materials are repaired usually when triggered by force,[21] thermal initiation,[16,22] photoinitiation[23–25] or pH.[26] Currently, reported underwater self-healing materials are mostly based on boronic acid derivatives[27,28] and catechol groups.[29,30] Relatively, there are few studies on the ability of microcapsule-type self-healing materials to self-heal underwater. In principle, amine-based curing agents or metal catalysts easily dissolve or get deactivated in the presence of water, and is a huge challenge that self-healing materials automatically heal underwater. Li *et al.*[31] microencapsulated isophorone diisocyanate (IPDI) and dispersed it in a coating that can bond the crack by immersion in water. Cho *et al.*[32] presented a self-healing material system based on polydimethylsiloxane to repair underwater. Among the materials, the fracture toughness repair rate is not more than 46% due to the difference between the core material and the matrix material, and the fracture toughness repair rate of healing is not more than 31% in water. In general, some cracks and the extent of self-repair are invisible to the naked eye during the self-healing process. Therefore, it is meaningful that the healing process of polymer materials be detected by observing

College of Chemistry and Life Science, Key Laboratory of Carbon Fiber Development and Application, Advanced Institute of Materials Science, Changchun University of Technology, Changchun 130012, Jilin Province, People's Republic of China. E-mail: xiaolinghan1981@163.com; liming15@ccut.edu.cn; Fax: +86-431-88499187; Tel: +86-431-85716471

† Electronic supplementary information (ESI) available. See DOI: 10.1039/d0ra03197f

Open Access Article. Published on 11 September 2020. Downloaded on 12/4/2025 4:19:03 PM.
This article is licensed under a Creative Commons Attribution-NonCommercial 3.0 Unported Licence.

the colour and fluorescent changes in the damaged area. Many researchers have developed various methods to detect the damage. Hamilton *et al.*[33] created a visual system to detect any mechanical damage by embedding two different colours into the self-healing materials. When the material was damaged, the two dyes mixed together to create a new colour. The average recovery of fracture toughness was 86% of the virgin sample fracture toughness. Song *et al.*[34] applied aggregation-induced emission (AIE), which is a unique phenomenon in which the emission intensity of a solid-state fluorescent dye is higher than that of the solution state, to detect the region of a coating undergoing self-healing. The degree of repair was determined by the degree of crack filling, and the damage was indicated by AIE. However, in many applications, simply filling or sealing crack does not meet the requirements of the overall material performance, and the recovery of fracture toughness strength is also crucial. In contrast to previous microcapsule-based materials, the damage indication we report here does not require any additional chromogenic agent. Instead, it is achieved by the fluorescent latent curing agents (FLCAs) in the matrix, which has both the damage indication function and the repair function.

In this work, a new kind of microcapsule-based self-healing material was designed. The principle of damage indication and self-healing is illustrated in Fig. 1. We used the same repair agent as the substrate to improve the repair rate. In order to avoid the failure of amine curing agents in humid environments, we blended FLCAs with the matrix. The latent curing agent was a Schiff base. In the presence of water, it hydrolyzes and releases amine groups to enable the cured epoxy repair agent self-repair. At the same time, a light-emitting substance with an aldehyde group is released to indicate the damage and damage repair. Therefore, the material has the ability to self-heal underwater and visualize the damage. In addition, it can not only repair the damaged region in water at room temperature but also detect the damage and the state of healing of the self-healing materials through two highly distinguishable colours under UV irradiation, which are visible to the naked eye. The influence of the addition of microcapsules and fluorescent latent curing agent on the self-healing properties and mechanical performance was also studied. Accordingly, self-healing materials that can be repaired underwater and have indications of damage are important application prospects for hydraulic engineering, environmental treatment engineering, underground concrete facilities, pipeline projects, and marine engineering.

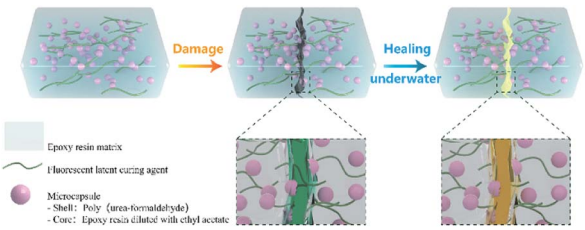

Fig. 1 Schematic of a self-healing material embedded with fluorescent latent curing agents and microcapsules.

2 Experimental part

2.1. Materials

Urea, an aqueous formaldehyde solution (37 wt%), resorcinol, ammonium chloride and 1-octanol were purchased from Aladdin Industrial Corporation. Ethyl acetate, ethanol, dichloromethane, chloroform and toluene were obtained from Tianjin Guangfu Fine Chemical Research Institute. Poly(ethylene-*alt*-maleic anhydride) (EMA Z-400, average molecular weight = 400 000) was gained from Guangzhou Haoyi Chemical Technology Co., Ltd. *m*-Xylylenediamine, diethylenetriamine, 2-(*N*-methylanilino)ethanol, triphenylphosphine and 1,4-phthalaldehyde were purchased from Shanghai Macklin Biochemical Co., Ltd. Diglycidyl ether of bisphenol – A (DGEBA E-51) epoxy resin was provided by Nantong Xingchen Synthetic Material Co Ltd. All chemicals and solvents were used without purification.

2.2. Microencapsulation of epoxy healing agents

Microencapsulation of epoxy healing agents was performed by a one-step method (ESI Fig. 2†). Urea (2.50 g), resorcinol (0.25 g) and ammonium chloride (0.25 g) were added to 0.5 wt% aqueous solution of EMA (100 mL). The pH of the solution was adjusted to 3.5 with 10% NaOH solution. One drop of 1-octanol was added to this solution to eliminate the surface bubbles. The resultant mixture was agitated at a stirring rate of 600 rpm. Meanwhile, a certain amount of an ethyl acetate solution of epoxy resin was slowly added to the mixture and stirred for 20 min to stabilize the emulsion. After adding 4.75 mL formaldehyde solution, the mixture was heated to 65 °C at a heating rate of 10 °C min^{-1}. The reaction was carried out at 65 °C for 4 h. After the polymerization reaction, the whole system was cooled down to room temperature and the obtained microcapsule was centrifuged and washed several times with ethanol and water. At last, the microcapsule was dried at 40 °C for 48 h.

The morphology of the microcapsules was observed using a scanning electron microscope (SEM), and the particle size distribution was measured using image analysis software (Nano Measurer). The composition of the microcapsules was characterized by Fourier transform infrared (FTIR) spectroscopy. A thermogravimetric analyzer (TGA) was used to analyze the thermal stability of the microcapsules in N_2 at a heating rate of 10 °C min^{-1}.

2.3. Synthesis of fluorescent dyes and fluoresce latent curing agents (FLCAs)

First, 2-(*N*-methylanilino)ethanol (1.51 g), triphenylphosphine (2.62 g), potassium iodide (1.66 g) and formaldehyde (0.81 g) were added into a three-necked flask and heated to 50 °C in an oil bath. Then, glacial acetic acid and chloroform were added and stirred at reflux for 50 h. After completion of the reaction, two layers of liquid appeared and the crude product was dissolved by adding chloroform. Subsequently, toluene was added to the mixture to precipitate a white solid, which was then filtered with suction to obtain a product. The terephthalic acid (1.34 g) and potassium *t*-butoxide (1.70 g) were dissolved in

Open Access Article. Published on 11 September 2020. Downloaded on 12/4/2025 4:19:03 PM.
This article is licensed under a Creative Commons Attribution-NonCommercial 3.0 Unported Licence.

dichloromethane and the mixture was stirred in a flask. The above product (5.38 g) was dissolved in dichloromethane and slowly added dropwise to the flask. After reacting at room temperature for 8 h, the fluorescent dye was obtained following extraction and recrystallization.

The fluorescent dye and *m*-xylylenediamine were separately dissolved in toluene, respectively. The fluorescent dye solution was heated to 120 °C, and the *m*-xylylenediamine solution was slowly added dropwise to the fluorescent dye solution and refluxed for 3 hours. After cooling to room temperature, the crude product was filtered off and washed three times with absolute ethanol. A small amount of dichloromethane was added to the crude product for heating reflux, followed by the addition of dichloromethane to completely dissolve the crude product and then the addition of ethanol to make the solution turbid. The product was cooled to room temperature, and the precipitated crystals were then filtered to obtain FLCAs.

2.4. Preparation of self-healing material samples

The TDCB (tapered double cantilever beam) fracture specimens (Fig. 2) were used to assess the healing performance. To prepare TDCB specimens, a certain amount of epoxy resin and diethylenetriamine were mixed uniformly in a proportion of 100 : 12, and then a percentage of FLCAs (the mass of the FLCA is 2%, 4%, 6%, and 8% of the mass of the epoxy resin mixture) and microcapsules (the mass of the microcapsules is 5%, 10%, 15%, and 20% of the mass of the epoxy resin mixture) were added under continuous stirring for 10 minutes. The compounds were degassed to remove entrapped air, and poured into a TDCB mold and cured at room temperature for 72 hours.

2.5. Lap-shear tests evaluating healing adhesion

To investigate the curing effect of FLCAs under wet conditions, a certain amount of microcapsule and a theoretical dosage of FLCA were stirred evenly. The mixture was applied to a steel tensile shear metal sheet, as shown in ESI Fig. 5.† The shear sheet was bonded in a water bath at room temperature for 7 days, and the tensile test was carried out using a universal testing machine. The average shear strength was reported based on 3 samples.

2.6. Evaluation of the healing efficiency

The TDCB test was performed using a universal testing machine (Z100, Zwick/Roell) to evaluate the effect of the content of FLCAs and microcapsules on the mechanical properties of the material. Prior to the mechanical testing, a crack was prearranged with a blade in the middle groove of the sample. The TDCB specimens were subjected to a tensile test using a universal force measuring machine at a displacement rate of 5 mm s^{-1}, and the virgin bending strength (P_C^{Virgin}) was obtained at the same time. The cracks of the specimens after TDCB test were fixed and put into water. The fractured specimens were completely repaired under different conditions, and then the bending strength (P_C^{Healed}) was obtained by reloading to failure. The repair rate (η) was defined as the ratio of the bending strength of the material after repaired (P_C^{Healed}) to virgin (P_C^{Virgin}). The calculation formula was calculated as follows:[35]

$$\eta = \frac{K_{IC}^{Healed}}{K_{IC}^{Virgin}} = \frac{P_C^{Healed}}{P_C^{Virgin}}$$

The average healing efficiency of each group was reported based on 5 specimens.

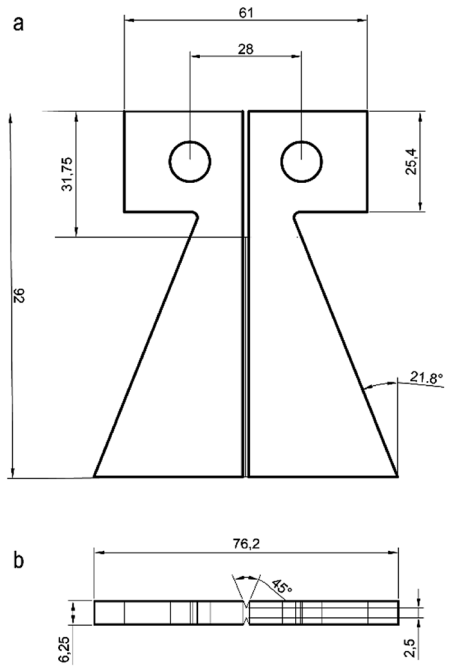

Fig. 2 (a) Top view of the TDCB spline. (b) Front view of the TDCB spline.

3 Results and discussion

3.1. Characterization of the latent curing agent

As shown in Fig. 3a, the FLCA was the latent curing agent that can decompose into a fluorescent dye and a curing agent (MXDA) by reacting with water. The formation of a fluorescent dye can cause a colour change in the material and produce a fluorescence colour change under ultraviolet light ($\lambda = 365$ nm). The functional groups of FLCAs and the fluorescent dyes were determined by infrared spectroscopy, as shown in Fig. 3b. For the FLCA (green curve), the wide absorption peaks of the curves centered at 3352 cm^{-1} corresponded to the O–H stretching vibration. The weak absorption peak at 2954 cm^{-1} was attributed to the C–H tensile vibration, the strong absorption peak at 1658 cm^{-1} was attributed to the deformation vibration of the C=N group, and the absorption peak at 1581 cm^{-1} was assigned to the C=C stretching vibration. For the fluorescent dye (yellow curve), two distinct absorption peaks at 3352 cm^{-1} and 1710 cm^{-1} were ascribed to the OH and C=O tensile vibration of the fluorescent dye.

The UV-vis spectra of FLCAs at different reaction times with water are shown in Fig. 3c. As the response time increased, the

Open Access Article. Published on 11 September 2020. Downloaded on 12/4/2025 4:19:03 PM.
This article is licensed under a Creative Commons Attribution-NonCommercial 3.0 Unported Licence.

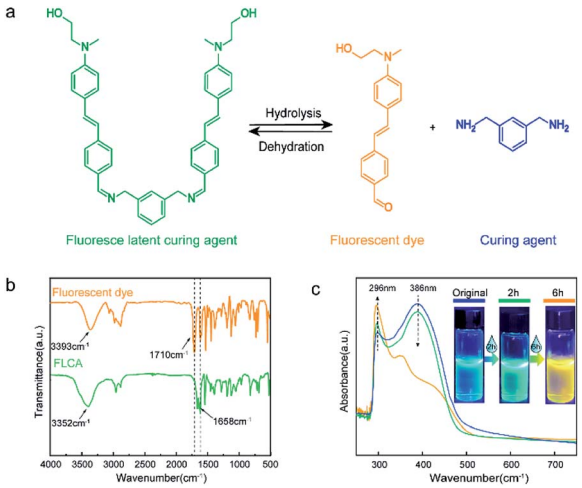

Fig. 3 (a) Structure and reversible reaction of the FLCA in the presence of water producing fluorescent dyes and MDXA. (b) FT-IR spectra of the FLCA and fluorescent dyes. (c) UV-vis spectrum of the FLCA (1×10^{-5} mol L^{-1}) in THF–H_2O (volume ratio 4 : 1) at different time points and the pictures under ultraviolet light ($\lambda = 365$ nm).

absorption peak of the FLCA at 386 nm decreased, but the absorption peak at 296 nm gradually increased, indicating that the FLCA underwent a hydrolysis reaction under the condition of water. Moreover, it was revealed that the FLCA overall emits blue fluorescence under ultraviolet light before the reaction. After contact with water, the fluorescent dye concentration increased and the fluorescence colour changed from blue to green and eventually turned yellow over time.

When the material is damaged, the crack extension causes the microcapsules to rupture. The FLCA in the matrix contacts the epoxy resin flowing out of the capsule. Under the action of water, the FLCA is hydrolysed to produce a fluorescent dye and a curing agent to achieve damage indication and damage. Therefore, to test whether the colour change of FLCAs in the epoxy resin is obvious, the epoxy resin and FLCA were mixed in a mass ratio of 2 : 1 and then dropped into a plastic crucible. As illustrated in ESI Fig. 6,† the colour change could be clearly observed in water with changes in time and temperature. The colour of the mixture changed from green to yellow, and the fluorescence colour changed from blue to yellow.

3.2. Preparation of microcapsules

Fig. 4a illustrates the structure of the microcapsule; epoxy resin was the core material and polyurea formaldehyde (PUF) was the shell material. FTIR was used to qualitatively characterize whether the epoxy polymer was successfully encapsulated in the microcapsules. Fig. 4b displays the FTIR spectra of the pristine epoxy resin, PUF-epoxy microcapsules and neat PU shell material. Specifically, the wide absorption peak exhibited at approximately 3100–3700 cm^{-1} corresponded to the N–H and O–H stretching vibration. The absorption peaks at 1669 cm^{-1} and 1572 cm^{-1} were attributed to the C=O and C–N stretching vibrations, respectively. The above-mentioned peaks confirmed that the PUF shell was successfully constructed by *in situ*

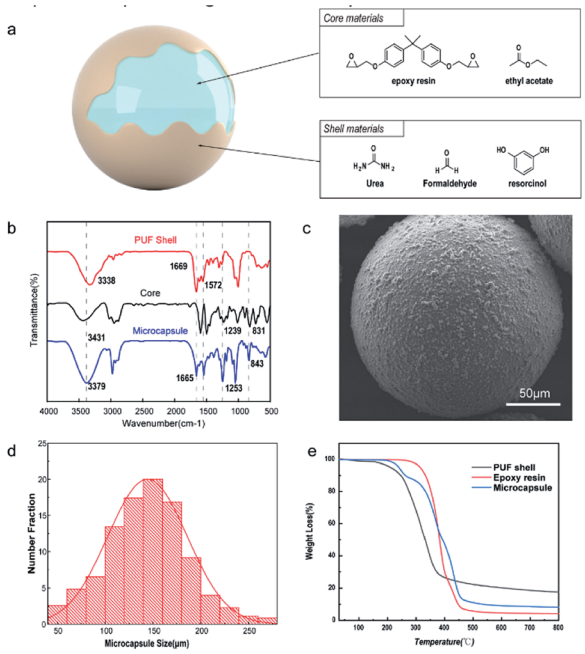

Fig. 4 (a) Structure of the microcapsule. (b) FTIR spectra of the PUF shell, core and microcapsule. (c) SEM micrograph of the microcapsule. (d) Histogram of the microcapsules' size distribution. (e) TGA curves of the PUF shell, epoxy resin and microcapsules.

polymerization. For the core material, the characteristic absorption peak at 3013 cm^{-1} denoted the stretching vibration of CH_2, and the appearance of the absorption peaks at 2923 cm^{-1} indicated the stretching vibration of $-CH_3$. The absorption peak observed at 1239 cm^{-1} denoted the stretching vibration of C–O–C. The characteristic absorption peaks observed at 915 cm^{-1} and 831 cm^{-1} were attributed to the epoxy group. Finally, all of the above characteristic peaks were matched in the spectrum of the microcapsule, which strongly verified that epoxy as a healing agent was successfully encapsulated in the PUF shell. As Fig. 4c shows, it was clearly observed that the shape of the microcapsules was a regular sphere, while the surface was rough, indicating that the shell of the microcapsules was produced by *in situ* deposition of PUF particles between the water and oil phase interfaces. The particle size distribution of the microcapsules is shown in Fig. 4d. The size of the microcapsules followed a normal distribution, and the average diameter was approximately 140 μm. In summary, these results indicated that the spherical microcapsules were synthesized successfully and did not leak out through the capsule wall.

The thermal stability of microcapsules is critical to their preservation and practical application. Consequently, the thermal performance of the PUF shell, epoxy resin and microcapsules was characterized by TGA. As shown in Fig. 4e, the PUF shell had a 5 wt% weight loss from 120 °C to 236 °C due to the decomposition of free formaldehyde absorbed on the surface of the microcapsules. In addition, the PUF shell began to decompose at 220 °C and completely decomposed at 600 °C. For the epoxy resin, almost no mass loss was observed at temperatures

Open Access Article. Published on 11 September 2020. Downloaded on 12/4/2025 4:19:03 PM.
This article is licensed under a Creative Commons Attribution-NonCommercial 3.0 Unported Licence.

below 298 °C. Through TG analysis of microcapsules, it was proven that the microcapsules have good thermal stability. In addition, the mass of the shell and solvent was 10.8%, the remaining mass was 11.0%, and the encapsulation percentage was 78.2% by calculation.

3.3. Optimization of the ratio of microcapsules and FLCAs in the self-healing material

To investigate the optimal self-healing performance, different mass percentages of FLCAs (2 wt%, 4 wt%, 6 wt%, and 8 wt%) and microcapsules (5 wt%, 10 wt%, 15 wt%, and 20 wt%) were dispersed in the epoxy matrix. The microcapsules and FLCAs were tested by lap-shear tests, and the average shear strength was 9.80 MPa (ESI Table 2†) in normal water for seven days. It was proved that the combination of FLCAs and epoxy resin microcapsule made the material self-healing underwater. As shown in Fig. 5a, when the content of the epoxy resin microcapsules was 5 wt%, the repair efficiency was much lower within the whole addition range of the latent curing agent. This is precisely because the epoxy resin released from the microcapsules could not sufficiently fill the crack, and the resin solidified to form a polymer with a small molecular weight. Furthermore, the self-healing efficiency increased with the increase in epoxy resin microcapsule content, suggesting that the issued epoxy resin might be adequately cured with FLCAs and led to a higher repair efficiency. In the case of 15 wt% microcapsules, the self-repair efficiency with a content of 6 wt% was almost the same as that with 8 wt% FLCA, indicating that too much latent hardener did not ensure the best degree of crosslinking. While the amount of microcapsules reached 20 wt%, the growth rate of the self-healing efficiency was very low, suggesting that 15 wt% microcapsules was able to effectively repair cracks and that the excessive content of microcapsules might lead to additional defect generation. In summary, considering that the content of epoxy resin microcapsules and FLCAs would dramatically affect the mechanical properties of the material, the optimal ratio was confirmed as 15% epoxy resin microcapsules and 6% FLCAs.

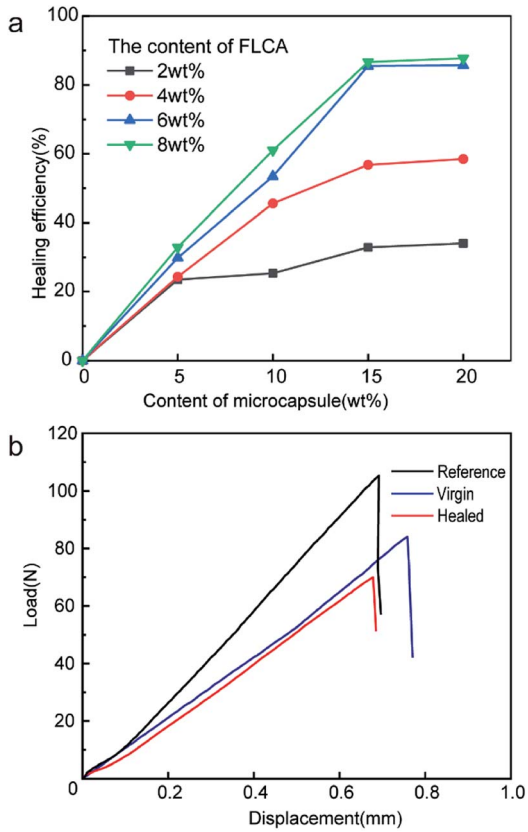

Fig. 5 (a) Influence of the content of FLCAs on the healing efficiency at different contents of FLCAs. (b) Load-displacement curves of the specimen with 15 wt% epoxy resin microcapsules and 6 wt% FLCAs.

3.4. Healing properties of the self-healing material at different temperatures

The healing efficiency of samples with 6 wt% latent curing agents and 15 wt% microcapsules repaired at different temperatures under water was discussed. As shown in Fig. 6, the materials could self-repair from 25 °C to 100 °C. As expected, the self-healing process at lower temperatures required more time, and the self-repair efficiency was accordingly reduced due to the high viscosity of the epoxy resin and the low solubility of FLCAs. With the increase in temperature, the solubility of FLCAs in the core material increased and accelerated the decomposition rate of FLCAs, thereby improving the self-repair efficiency. However, further increasing the temperature beyond 60 °C caused gradual evaporation of ethyl acetate in the microcapsule and made FLCAs difficult to dissolve. Moreover, it decreased the amount of FLCAs in contact with the epoxy polymer, thereby reducing the degree of curing and the self-repair efficiency. Over sufficient time, the healing efficiency at 25 °C and 100 °C is lower than that at 60 °C, mainly due to the poor fluidity of the epoxy resin in the microcapsules at normal temperatures, resulting in defects in the healing area. According to Fig. 7, the healing efficiency was 83.5% ± 9.4 after healing at 60 °C for 4 h, which was similar to the healing efficiency (85.6% ± 10.2%) of the material healed at 60 °C, confirming that the epoxy resin in the microcapsules healed at 60 °C for 4 h was substantially cured.

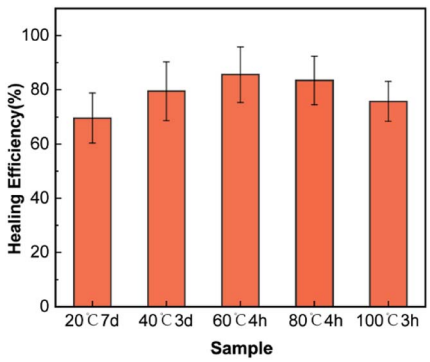

Fig. 6 Healing efficiency of the samples healed at different temperatures.

Open Access Article. Published on 11 September 2020. Downloaded on 12/4/2025 4:19:03 PM.
This article is licensed under a Creative Commons Attribution-NonCommercial 3.0 Unported Licence.

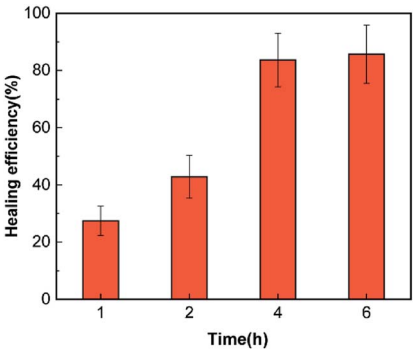

Fig. 7 Healing efficiency of the samples healed at 60 °C for different time periods in water.

3.5. Detection of different fluorescence colours and visible colours from cracked and healed regions

In general, the ability to detect a change in fluorescence colours with regard to damage and healing in the self-healing field could allow the monitoring of surface conditions and prevent material damage. The epoxy sample with 15% microcapsules and 8% FLCAs embedded was fractured using a universal testing machine (Z100, Zwick/Roell) and imaged using a digital camera (D7000, NIKON), an optical microscope and a scanning electron microscope (ISM-7610F, JEOL). As shown in Fig. 8, the crack could be clearly observed in the image before and after the repair of the self-healing material, and the width was approximately 20 μm. In Fig. 8a-1 and a-2, the colour of the cracked area before healing under visible light was green. After repairing in water at 60 °C, the epoxy filled the crack, and the damaged region turned yellow. To confirm that the scratching and healing region yielded different fluorescence colours, the cracks were observed under UV irradiation. Before healing, the fluorescence colour of the cracked area did not change in Fig. 8b-1. After healing, the crack region produced obvious yellow fluorescence in Fig. 8b-2. As shown in Fig. 8c-1 and c-2, the SEM image shows that the crack healing area was completely healed and the interface was smooth. Therefore, not only the designed material can detect the position of crack generation under ultraviolet light, but the change in the crack can also be observed under visible light.

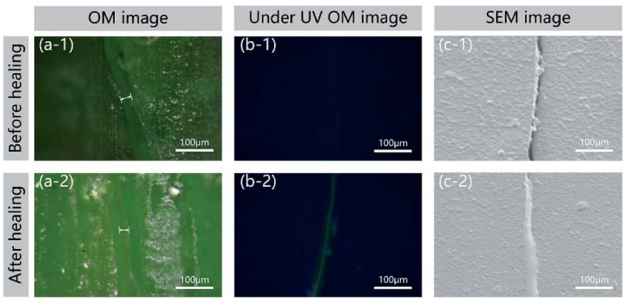

Fig. 8 (a-1) OM image of the material before healing. (a-2) OM image of the material after repair. (b-1) OM image of material under UV light before healing ($\lambda = 365$ nm). (b-2) OM image of the material under UV light ($\lambda = 365$ nm) after healing. (c-1) SEM image of the material before healing. (c-2) SEM image of the material after healing.

4 Conclusions

In this work, the microcapsule-type self-healing system successfully used changes in visible colours and fluorescence colours to detect cracks and healed regions. In addition, the material can self-repair from 25 °C to 100 °C due to the hydrolysis of FLCAs into a fluorescent agent and a curing agent. The optimum content of epoxy resin microcapsules was determined to be 15%, and the optimal FLCA content was 6%. When the material was damaged by an external force, it could be repaired in water at 60 °C for 4 h, and the healing efficiency reached 85.6%. Additionally, the fluorescence colour changed to yellow after repairing the crack region, and the degree of self-repair could be judged by the change in colour.

Conflicts of interest

There are no conflicts to declare.

Acknowledgements

This work was supported by the National Natural Science Foundation of China (Grant No. 51603020, 21644003, 21704006), the Natural Science Foundation of Jilin Province (Grant No. 20190201280JC, 20180101193JC).

References

1 X. Zheng, Q. Wang, Y. Li, J. Luan and N. Wang, Microcapsule-Based Visualization Smart Sensors for Damage Detection: Principles and Applications, *Adv. Mater. Technol.*, 2019, **5**, 1900832, DOI: 10.1002/admt.201900832.
2 T. P. Huynh, M. Khatib and H. Haick, Self-Healable Materials for Underwater Applications, *Adv. Mater. Technol.*, 2019, **4**, 1900081, DOI: 10.1002/admt.201900081.
3 E. T. Thostenson and T. W. Chou, Carbon Nanotube Networks: Sensing of Distributed Strain and Damage for Life Prediction and Self Healing, *Adv. Mater.*, 2006, **18**, 2837–2841, DOI: 10.1002/adma.200600977.
4 J. Pang and I. Bond, 'Bleeding composites'—damage detection and self-repair using a biomimetic approach, *Composites, Part A*, 2005, **36**(2), 183–188, DOI: 10.1016/j.compositesa.2004.06.016.
5 T. J. Swait, A. Rauf, R. Grainger, P. B. Bailey, A. D. Lafferty, E. J. Fleet, R. J. Hand and S. A. Hayes, Smart composite materials for self-sensing and self-healing, *Plast., Rubber Compos.*, 2012, **41**(4/5), 215–224, DOI: 10.1179/1743289811Y.0000000039.
6 M. Kosarli, D. G. Bekas, K. Tsirka, D. Baltzis, D. T. Vaimakis-Tsogkas, S. Orfanidis, G. Papavassiliou and A. S. Paipetis, Microcapsule-based self-healing materials: Healing efficiency and toughness reduction vs. capsule size, *Composites, Part B*, 2019, **171**, 78–86, DOI: 10.1016/j.compositesb.2019.04.030.

Open Access Article. Published on 11 September 2020. Downloaded on 12/4/2025 4:19:03 PM.
This article is licensed under a Creative Commons Attribution-NonCommercial 3.0 Unported Licence.

7 M. W. Lee, S. An, S. S. Yoon and A. L. Yarin, Advances in self-healing materials based on vascular networks with mechanical self-repair characteristics, *Adv. Colloid Interface Sci.*, 2018, **252**, 21–37, DOI: 10.1016/j.cis.2017.12.010.

8 S. Y. Kim, N. R. Sottos and S. R. White, Self-healing of fatigue damage in cross-ply glass/epoxy laminates, *Compos. Sci. Technol.*, 2019, **175**, 122–127, DOI: 10.1016/j.compscitech.2019.03.016.

9 I. L. Hia, V. Vahedi and P. Pasbakhsh, Self-healing polymer composites: prospects, challenges, and applications, *Polym. Rev.*, 2016, **56**(2), 225–261, DOI: 10.1080/15583724.2015.1106555.

10 H. Zhang, X. Zhang, C. Bao, X. Li, F. Duan, K. Friedrich and J. Yang, Skin-Inspired, Fully Autonomous Self-Warning and Self-Repairing Polymeric Material under Damaging Events, *Chem. Mater.*, 2019, **31**(7), 2611–2618, DOI: 10.1021/acs.chemmater.9b00398.

11 A. Boger, P. Heini, M. Windolf and E. Schneider, Adjacent vertebral failure after vertebroplasty: a biomechanical study of low-modulus PMMA cement, *Eur. Spine J.*, 2007, **16**(12), 2118–2125, DOI: 10.1007/s00586-007-0473-0.

12 M. M. C. Dailey, A. W. Silvia and P. J. McIntire, A self-healing biomaterial based on free-radical polymerization, *J. Biomed. Mater. Res., Part A*, 2013, **102**(9), DOI: 10.1002/jbm.a.34975.

13 Y. Cao, H. Wu, S. Allec and B. Wong, A Highly Stretchy, Transparent Elastomer with the Capability to Automatically Self-Heal Underwater, *Adv. Mater.*, 2018, **30**(49), 1804602, DOI: 10.1002/adma.201804602.

14 S. Y. Kim, A. R. Jones, N. R. Sottos and S. R. White, Manufacturing of unidirectional glass/epoxy prepreg with microencapsulated liquid healing agents, *Compos. Sci. Technol.*, 2017, **153**, 190–197, DOI: 10.1016/j.compscitech.2017.10.017.

15 S. R. White, N. R. Sottos, P. H. Geubelle, J. S. Moore, M. R. Kessler, S. Sriram, E. Brown and S. Viswanathan, Autonomic healing of polymer composites, *Nature*, 2001, **409**(6822), 794, DOI: 10.1038/35057232.

16 T. Yin, M. Z. Rong, M. Q. Zhang and G. C. Yang, Self-healing epoxy composites–preparation and effect of the healant consisting of microencapsulated epoxy and latent curing agent, *Compos. Sci. Technol.*, 2007, **67**(2), 201–212, DOI: 10.1016/j.compscitech.2006.07.028.

17 S. H. Cho, H. M. Andersson, S. R. White, N. R. Sottos and P. V. Braun, Polydimethylsiloxane-based self-healing materials, *Adv. Mater.*, 2006, **18**(8), 997–1000, DOI: 10.1002/adma.200501814.

18 A. Yabuki, Self-healing coatings for corrosion inhibition of metals, *Mod. Appl. Sci.*, 2015, **9**(7), 214, DOI: 10.5539/mas.v9n7p214.

19 L. M. Meng, Y. C. Yuan, M. Z. Rong and M. Q. Zhang, A dual mechanism single-component self-healing strategy for polymers, *J. Mater. Chem.*, 2010, **20**(29), 6030–6038, DOI: 10.1039/C0JM00268B.

20 M. Huang and J. Yang, Facile microencapsulation of HDI for self-healing anticorrosion coatings, *J. Mater. Chem.*, 2011, **21**(30), 11123–11130, DOI: 10.1039/C1JM10794A.

21 C. Calvino, A. Guha, C. Weder and S. Schrettl, Self-Calibrating Mechanochromic Fluorescent Polymers Based on Encapsulated Excimer-Forming Dyes, *Adv. Mater.*, 2018, **30**(19), 1704603, DOI: 10.1002/adma.201704603.

22 D. Y. Wu, S. Meure and D. Solomon, Self-healing polymeric materials: A review of recent developments, *Prog. Polym. Sci.*, 2008, **33**(5), 479–522, DOI: 10.1016/j.progpolymsci.2008.02.001.

23 Y. K. Song, T. H. Lee, J. C. Kim, K. C. Lee, S.-H. Lee, S. M. Noh and Y. I. Park, Dual Monitoring of Cracking and Healing in Self-healing Coatings Using Microcapsules Loaded with Two Fluorescent Dyes, *Molecules*, 2019, **24**(9), 1679, DOI: 10.3390/molecules24091679.

24 W. Guo, Y. Jia, K. Tian, Z. Xu, J. Jiao, R. Li, Y. Wu, L. Cao and H. Wang, UV-triggered self-healing of a single robust SiO_2 microcapsule based on cationic polymerization for potential application in aerospace coatings, *ACS Appl. Mater. Interfaces*, 2016, **8**(32), 21046–21054, DOI: 10.1021/acsami.6b06091.

25 Y. Zhu, K. Cao, M. Chen and L. Wu, Synthesis of UV-Responsive Self-Healing Microcapsules and Their Potential Application in Aerospace Coatings, *ACS Appl. Mater. Interfaces*, 2019, **11**(36), 33314–33322, DOI: 10.1021/acsami.9b10737.

26 B. Dong, Y. Wang, G. Fang, N. Han, F. Xing and Y. Lu, Smart releasing behavior of a chemical self-healing microcapsule in the stimulated concrete pore solution, *Cem. Concr. Compos.*, 2015, **56**, 46–50, DOI: 10.1016/j.cemconcomp.2014.10.006.

27 W. P. Chen, D. Z. Hao, W. J. Hao, X. L. Guo and L. Jiang, Hydrogel with Ultrafast Self-Healing Property Both in Air and Underwater, *ACS Appl. Mater. Interfaces*, 2017, **10**(1), 1258, DOI: 10.1021/acsami.7b17118.

28 C. Kim, H. Ejima and N. Yoshie, Non-swellable self-healing polymer with long-term stability under seawater, *RSC Adv.*, 2017, **7**(31), 19288–19295, DOI: 10.1039/C7RA01778B.

29 C. C. Deng, W. L. A. Brooks, K. A. Abboud and B. S. Sumerlin, Boronic Acid-Based Hydrogels Undergo Self-Healing at Neutral and Acidic pH, *ACS Macro Lett.*, 2015, **4**(2), 220–224, DOI: 10.1021/acsmacrolett.5b00018.

30 B. K. Ahn, W. L. Dong, J. N. Israelachvili and J. H. Waite, Surface-initiated self-healing of polymers in aqueous media, *Nat. Mater.*, 2014, **13**(9), 867–872, DOI: 10.1038/nmat4037.

31 C. Li, J. Tan, J. Gu, Q. Lei, B. Zhang and Q. Zhang, Rapid and efficient synthesis of isocyanate microcapsules via thiol-ene photopolymerization in Pickering emulsion and its application in self-healing coating, *Compos. Sci. Technol.*, 2016, **123**(4), 250–258, DOI: 10.1016/j.compscitech.2016.01.001.

32 S. H. Cho, H. M. Andersson, S. R. White, N. R. Sottos and P. V. Braun, Polydimethylsiloxane-Based Self-Healing Materials, *Adv. Mater.*, 2010, **18**(8), 997–1000, DOI: 10.1002/adma.200501814.

33 A. R. Hamilton, N. R. Sottos and S. R. White, Self-healing of internal damage in synthetic vascular materials, *Adv. Mater.*, 2010, **22**(45), 5159–5163, DOI: 10.1002/adma.201002561.

Open Access Article. Published on 11 September 2020. Downloaded on 12/4/2025 4:19:03 PM.
This article is licensed under a Creative Commons Attribution-NonCommercial 3.0 Unported Licence.

34 Y. K. Song, B. Kim, T. H. Lee, S. Y. Kim, J. C. Kim, S. M. Noh and Y. I. Park, Monitoring fluorescence colors to separately identify cracks and healed cracks in microcapsule-containing self-healing coating, *Sens. Actuators, B*, 2018, **257**, 1001–1008, DOI: 10.1016/j.snb.2017.11.019.

35 H. Jin, C. L. Mangun, D. S. Stradley, J. S. Moore, N. R. Sottos and S. R. White, Self-healing thermoset using encapsulated epoxy-amine healing chemistry, *Polymer*, 2012, **53**(2), 581–587, DOI: 10.1016/j.polymer.2011.12.005.

 This journal is © The Royal Society of Chemistry 2020